Gaussian Beam Modeling for Commercial Transducers Applied to Aero Engine Disk Inspection

Martin SPIES, Fraunhofer-Institut Zerstörungsfreie Prüfverfahren (IZFP),
Universität des Saarlandes, Saarbrücken, Germany

Abstract. Gaussian beam superposition is applied to model representative standard transducers, which are used in aero engine disk inspection. Previously published approaches available in the literature have been applied and modified to account for rectangular and non-planar transducer apertures. Beam field calculation for both single and layered media is addressed.

Introduction

Beam field modeling using the superposition of Gaussian beams (GB) is highly efficient due to the low computation times. Thus, respective simulations allow for a fast evaluation of even complex inspection situations. In this paper, an extension of the GB method is presented, addressing the simulation of circular and rectangular, flat and focused transducers. In this approach, a small number of GBs is required to synthesize the transducer beam field. While the usual approach to determine the coefficients characterizing the beams is based on a numerically expensive least-squares optimization [1], an efficient approach can be found in literature, which replaces iterative optimization by a polynomial root-finding problem [2]. It can be applied to field profile data obtained at the near-field length of flat transducers or in the focal point of focused transducers.

Here, these reference profiles are determined using the point source superposition technique (GPSS) which is exact as far as the modeling of transducer-generated beam fields is concerned [3]. For modeling rectangular transducers, a formulation recently presented in the literature [4] is applied and further modified with respect to focused transducers. To illustrate the efficiency of the extended Gaussian beam superposition technique (GBS) the monochromatic beam fields of various commercial transducers are presented in comparison with exact GPSS results. The method is then applied to disk geometries of interest in turbine engine component inspection using commercial transducers and immersion technique. Computationally efficient transient modeling by superposition of 'temporally limited' GBs has been developed recently [5] and is also illustrated.

1. Gaussian Beam Modeling -Theory

1.1 Basic Relationships

For a general homogeneous medium, the particle displacement vector of a single Gaussian beam of wavetype α can be represented according to

$$\underline{u}_\alpha(\underline{R}) = U\,\hat{\underline{u}}_\alpha \exp\left[j\underline{K}_\alpha \cdot (\underline{R}-\bar{\underline{R}})\right] \cdot \left[\frac{\det \underline{\underline{M}}_\alpha}{\det \underline{\underline{M}}_0}\right]^{\frac{1}{2}} \exp\left[j\omega\frac{1}{2}(\underline{R}-\bar{\underline{R}})\cdot \underline{\underline{M}}_\alpha \cdot (\underline{R}-\bar{\underline{R}})\right], \quad (1)$$

where $\bar{\underline{R}}$ is along the central ray (parallel to the group velocity vector $\underline{c}_\alpha$), $\underline{K}_\alpha = K_\alpha\ \hat{\underline{K}}$ ($\hat{\underline{K}}$ being the phase direction) and $\hat{\underline{u}}_\alpha$ is the polarization vector; its envelope is characterized by the complex matrix

$$\underline{\underline{M}}_\alpha(\underline{R}) = \underline{\underline{M}}_0 \cdot \left[\underline{\underline{I}} + \frac{\underline{R}\cdot\hat{\underline{K}}}{\underline{c}_\alpha\cdot\hat{\underline{K}}}\left(\underline{\underline{N}}_\alpha \cdot \underline{\underline{M}}_0\right)\right]^{-1}. \quad (2)$$

The envelope matrix at $\underline{R}=\underline{0}$ contains the beam waist parameter M according to

$$\underline{\underline{M}}_0 = M\left(\underline{\underline{I}} - \hat{\underline{K}}\hat{\underline{K}}\right), \quad (3)$$

and the evolution of $\underline{\underline{M}}_0$ (Eq. (2)) is governed by the real-valued matrix $\underline{\underline{N}}_\alpha = \partial\underline{c}_\alpha/\partial\underline{K}$, accounting for the geometrical spreading of the beam [6].

Considering beam transmission through an interface according to Fig. 1, a similar description holds according to

$$\begin{aligned}\underline{u}^{T\alpha}(\underline{R}) &= U^{T\alpha}(\underline{R}_0)\,\hat{\underline{u}}^{T\alpha}\exp\left[j\underline{K}^{T\alpha}\cdot(\underline{R}-\bar{\underline{R}}^{T\alpha})\right]\left[\frac{\det \underline{\underline{M}}^{T\alpha}}{\det \underline{\underline{M}}^{T\alpha}(\underline{R}_0)}\right]^{\frac{1}{2}} \\ &\cdot\exp\left[j\omega\frac{1}{2}(\underline{R}-\bar{\underline{R}}^{T\alpha})\cdot\underline{\underline{M}}^{T\alpha}\cdot(\underline{R}-\bar{\underline{R}}^{T\alpha})\right], \end{aligned} \quad (4)$$

with $\underline{R}_0$ designating the position where the incident beam hits the interface, $U^{T\alpha}$ is the (plane wave) transmission coefficient and $\bar{\underline{R}}^{T\alpha}$ represents the central ray path of the transmitted beam. The complex envelope matrix is given by

$$\underline{\underline{M}}^{T\alpha} = \underline{\underline{M}}^{T\alpha}(\underline{R}_0)\cdot\left[\underline{\underline{I}} + \left(\frac{\underline{R}\cdot\hat{\underline{K}}^{T\alpha}}{\underline{c}^{T\alpha}\cdot\hat{\underline{K}}^{T\alpha}} - \frac{\underline{R}_0\cdot\hat{\underline{K}}^{I}}{\underline{c}^{I}\cdot\hat{\underline{K}}^{I}}\right)\underline{\underline{N}}^{T\alpha}\cdot\underline{\underline{M}}^{T\alpha}(\underline{R}_0)\right]^{-1}. \quad (5)$$

The transformation of the envelope matrix $\underline{\underline{M}}^I$ of the incident beam to the transmitted one is performed according to

$$\begin{aligned}\underline{\underline{M}}^{T\alpha}(\underline{R}_0) &= \left(\underline{\underline{S}}^{T\alpha-1}\cdot\underline{\underline{S}}^{I}\right)\cdot\underline{\underline{M}}^{I}(\underline{R}_0)\cdot\left(\underline{\underline{S}}^{T\alpha-1}\cdot\underline{\underline{S}}^{I}\right)^{T} \\ &+ 2\omega^{-1}\underline{t}_z\cdot(\underline{K}^{I}-\underline{K}^{\alpha})\left(\underline{\underline{Q}}^{T\alpha-1}\right)\cdot\underline{\underline{D}}\cdot\left(\underline{\underline{Q}}^{T\alpha-1}\right)^{T}, \end{aligned} \quad (6)$$

Where the $\underline{\underline{S}}$-and $\underline{\underline{Q}}$-transformation matrices depend on the tractions $\underline{t}_x$, $\underline{t}_y$ and $\underline{t}_z$ at the interface, $\underline{\underline{D}}$ contains the local radii of curvature of a curved component. In Ref. [6}, these relationships have been derived for the case of Gaussian wave packets, which can be regarded as Gaussian beams of finite length along the central ray. Thus, the relationships can be applied correspondingly.

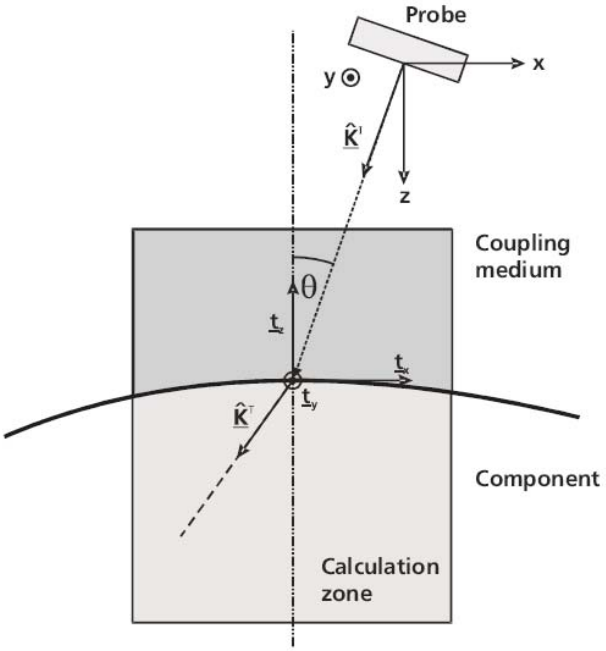

Figure 1. Principal set-up of probe, component and the coordinate system in considering the transmission problem in view of immersion testing.

1.2 GB Superposition For Circular and Rectangular Transducers

Introducing isotropic material conditions and setting $\underline{\hat{K}} = \underline{e}_z$ yields

$$\underline{\underline{M}}_{\alpha}^{iso} = \frac{M}{v_\alpha(1 + M v_\alpha z)} \, (\underline{\underline{I}} - \underline{e}_z \, \underline{e}_z) \, , \tag{7}$$

where v_α designates the phase velocity. With $r^2 = x^2 + y^2$, the beam field of a circular piston in a single medium can be formulated as a superposition of N beams according to

$$| \, \underline{u}_{\alpha}^{circ}(\underline{R}) \, | = \sum_{n=1}^{N} \frac{U_n}{1 + M_n v_\alpha z} \exp\left[j\omega \, \frac{M_n \, r^2}{2(1 + M_n v_\alpha \, z)} \right] , \tag{8}$$

where the complex amplitudes U_n and the beam waist parameters M_n characterize the individual beams. Equation (8) can be directly compared with the formulation given by Wen & Breazeale (W&B) in [1]

$$\phi(r, z) = \frac{j}{k} \sum_{n=1}^{N} \frac{A_n}{B_n + (2j/k)z} \exp\left[-\frac{r^2}{B_n + (2j/k)z} \right] \, , \tag{9}$$

to provide the following relationships for the respective coefficients ($k = \omega/v$)

$$\begin{aligned} U_n &= A_n / B_n \, , \\ M_n &= 2j/(\omega B_n) \, . \end{aligned} \tag{10}$$

In modeling rectangular transducers, a formulation given in [4] can be applied, which reduces the Fresnel field integral to the superposition of a set of two-dimensional Gaussian beams. A rectangular piston transducer of side lengths a and b is thus described according to

$$|\,\underline{u}_{\alpha}^{rect}(\underline{R})\,| \;=\; \sum_{n=1}^{N} \frac{U_n^x}{\sqrt{1+M_n^x v_\alpha z}} \exp\left[\mathrm{j}\omega\,\frac{M_n^x\,x^2}{2(1+M_n^x v_\alpha\,z)}\right] \cdot \sum_{n=1}^{N} \frac{U_n^y}{\sqrt{1+M_n^y v_\alpha z}} \exp\left[\mathrm{j}\omega\,\frac{M_n^y\,y^2}{2(1+M_n^y v_\alpha\,z)}\right]. \qquad (11)$$

Here, $U_n^{x,y}$ and $M_n^{x,y}$ are sets of coeffcients characterizing circular piston transducers of diameters *a* and *b*, respectively.

While the authors of [4] rely on the W&B coeffcients, the results presented here were obtained using two different sets of coeffcients, individually determined in view of the transducers under concern. The usual approach to determine GB coeffcients is based on a numerically expensive least-squares optimization, while in [2] an effcient approach has been presented based on a classical signal processing technique, known as Prony's method. This approach replaces iterative optimization by a polynomial root-finding problem. It has been implemented and applied to field profile data obtained at the near-field length of flat transducers or in the focal point of focused transducers.

The calculation of transducer beam fields transmitted through an interface is based on a straight forward integration of Eqs. (4) to (6) into Eqs. (10) and (11), respectively.

1.3 Gaussian Beam Transient Modeling

A transient modeling procedure has recently been elaborated, which circumvents intensive calculations in frequency domain [5]. The implemented algorithm operates in time domain and has been inferred from Gaussian wave packet (GWP) theory. The relation between GBs and GWPs is a very basic one: GBs can be thought of as being GWPs with infinite extension along the central ray. Thus, GB theory can be transferred into GWP theory by adding an additional parameter to account for the pulse length.

Based on these relationships, transient modeling is performed by superposition of GWPs. This approach is most advantageous, since no major changes in the subsequent formulations given in the previous paragraphs have to be performed. The formulations to be used for the layered and/or anisotropic cases can be found in [7].

2. Numerical Evaluation

The effciency of the extended Gaussian beam superposition technique (GBS) is illustrated by beam field results obtained for two commercial transducers, which are applied in turbine engine disk inspection [8]:

- Probe 1: circular aperture, 10 MHz frequency, 12.7 mm diameter, focal length 101.6 mm in water (Harisonic I3-1008R),
- Probe 2: rectangular aperture, 15 MHz frequency, dimensions 7.9 x 4.75 mm², cylindrical focus at 63.5 mm in water (Harisonic I2LRA).

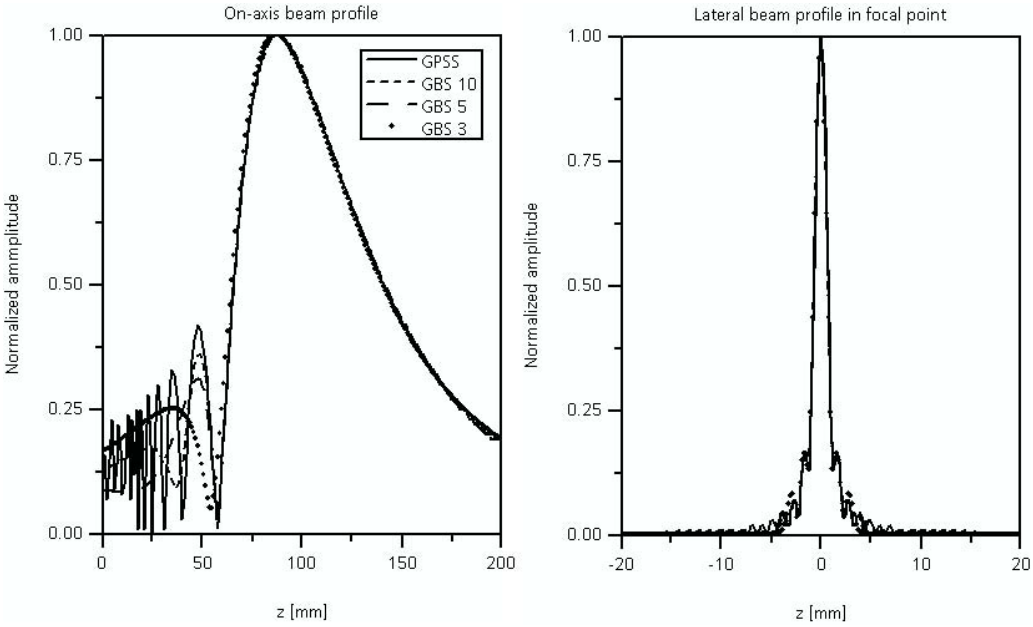

Figure 2. On-axis and lateral beam profile in the focal point for Probe 1 (in water), calculated using point source superposition (GPSS) and Gaussian beam superposition for a three-, five-and ten-term solution.

2.1 Determination of GB Coeffcient Sets

The reference profiles used in evaluating the GB coeffcients individually for each transducer are determined using the point source super position technique (GPSS) which is exact as far as the modeling of transducer-generated beam fields in homogeneous media is concerned [3]. While the W&B coeffcients have been determined for a prescribed amplitude distribution within the transducer aperture [1], the procedure applied here is based on the profiles at the transducer near-field/focal length. Thus, these reference profiles include side lobe structure information, so that the number of Gaussian beams necessary for an appropriate description of the beam field can be reduced to less than ten (W&B case). This is illustrated in Fig. 2, where the on-axis and the lateral field profiles are displayed for Probe 1. The solid curve represents the exact GPSS calculation while the dashed and dotted curves show the calculation results obtained using a superposition of 3, 5 and 10 Gaussian beams, respectively, with three different sets of coeffcients determined accordingly. Noticable, but negligible differences exist in the near-field structure and in the outer side lobe structure.

2.2 Transducer Beam Fields in Water and Titanium

To illustrate the effciency of the presented GBS approach, in the following (monochromatic) beam field profiles of Probe 2 are shown, which is a line focusing probe with a cylindrically curved, rectangular aperture. Applying a superposition of five GBs on the basis of Eq. (11), the two sets of coeffcients used are the ones obtained for circular piston transducers with diameters corresponding to the side lengths of Probe 2, respectively, one of them being flat and one of them being spherically curved with a radius of curvature of 63.5 mm. Figure 3 displays the axial and the two lateral profiles

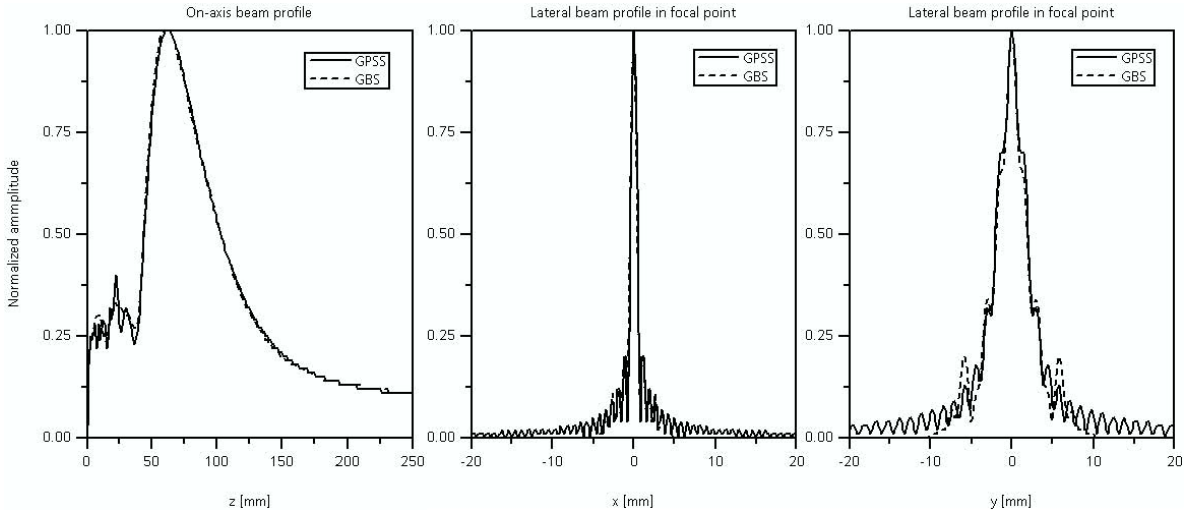

Figure 3. On-axis and lateral beam profiles in the focal plane (center) and perpendicular to it (right) in the focal distance for Probe 2 (in water), calculated using point source superposition (GPSS) and Gaussian beam superposition (5 beams).

(in the focal plane and perpendicular to it). Again the GBS results agree excellently with the exact GPSS results.

In view of immersion testing of aero engine components, the inspection of a titanium disk from the inner bore is addressed, where the inner bore diameter is 34 mm. Although the GB approach of modeling beam transmission through this strongly curved interface employs a paraxial approximation -the central beam being supplied with the corresponding (plane wave) transmission coefficient and the local radii of curvature of the component surface - the results compare well with the results obtained using the far more sophisticated point source superposition technique. In Figure 4, the on-axis and lateral

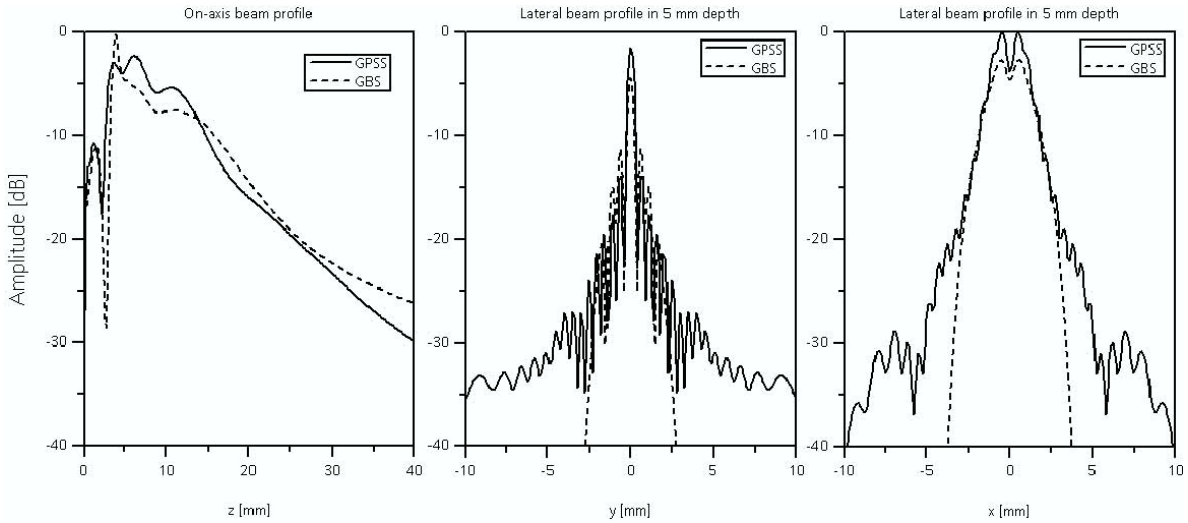

Figure 4. On-axis and lateral beam profiles in the focal plane (center) and perpendicular to it (right) in 5 mm depth of the titanium disc, calculated forProbe 2 using point source superposition(GPSS) and Gaussian beam superposition (5 beams).

profiles are plotted at a depth of 5 mm in the titanium disc, using logarithmic scaling. Major differences between the two calculation methods only exist below an amplitude level of -20 dB. Thus, the GBS method can be considered as an efficient tool for simulating ultrasonic inspection of complex shaped components.

50 % bandwidth

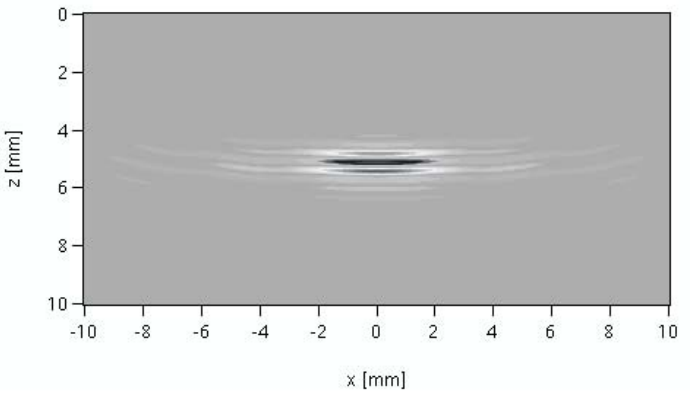

75 % bandwidth

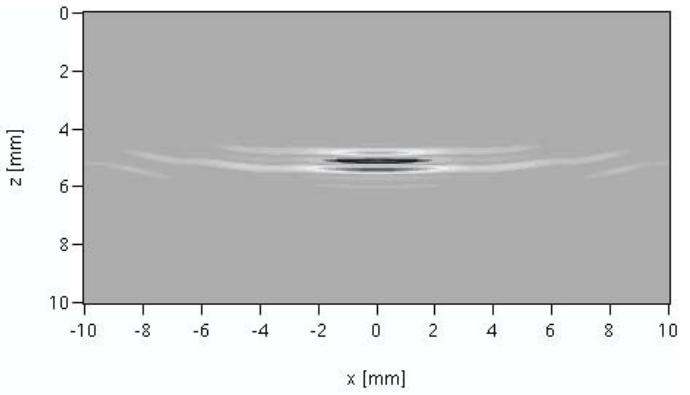

50 % bandwidth

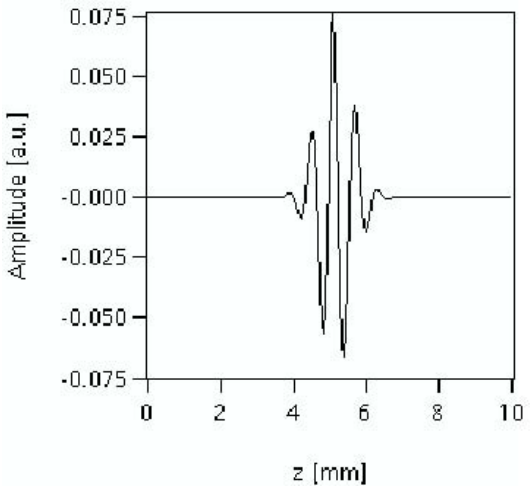

75 % bandwidth

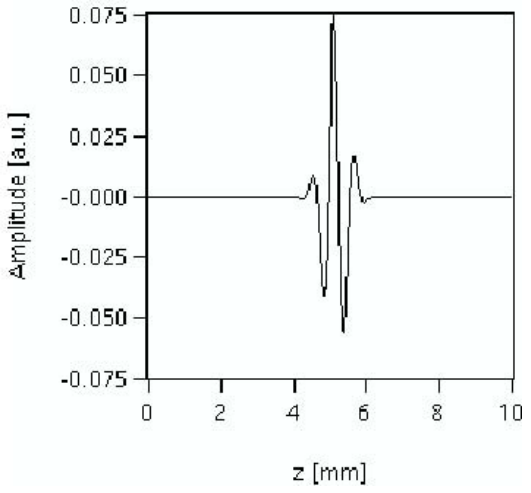

Figure 5. Wave propagation snapshots within a planar titanium specimen (top); representation of the wave forms at x = 0mm (bottom) for Probe 2.

2.3 Transient Modeling -Wavefront Images

To demonstrate the transient GB approach, the insonification into a planar component using immersion technique (100 mm water path) has been addressed for Probe 2. Figure 5 shows the images of the transient wave fronts generated in the component at 68.4 µs, where signals of 50 % and 75 % bandwidth have been modeled.

3. Summary

The presented results show that GBS modeling yields reliable results at low computation times. The calculation times are tremendously lower as compared to other methods, which is particularly beneficial at higher frequencies, as of special interest in high resolution NDT of aero engine components. The Gaussian beam results are obtained instantaneously, while the point source superposition results are calculated within three to four minutes on a 3 GHz Intel Xeon PC. This speed-up in calculation time is particularly useful in performing transient calculations. The transient approach is also extremely fast, since it operates in time domain and preserves the computational effciency of the monochromatic approach. A sequence of 50 snapshots (see Fig. 5) –as an example –has been calculated for a spatial discretisation of 200 by 200 points within less than 10 seconds. Differences of this 'pseudo-transient' approach in comparison with a frequency domain approach exist in the near-field, since the near-field structure of the monochromatic beam field is conserved. However, relevant evaluations are mostly done in the far-field. Also, the GB module provides a fast apriori evaluation of an inspection situation, while more exact methods can be subsequently applied, if necessary. Finally, the effciency of Prony's method in determining new sets of GB coeffcients is beneficial in view of setting up a data base for commercial/standard type transducers. Validation of the GBS approach has been performed with respect to NDT of aeroengine components [8].

Acknowledgment

This work has been funded by the European Commission under Contract Nº G4RD-CT-2002-00860, which is gratefully acknowledged. The information in this document is provided as is and no guarantee or warranty is given that the information is fit for any particular purpose. The user thereof uses the information at its sole risk and liability.

References

[1] Wen, J.J., Breazeale, M.A., *J. Acoust. Soc. Am*. **83**, 1752-1756 (1988)
[2] Prange, M.D., Shenoy, R.G., *Ultrasonics* **34**, 117-119 (1996)
[3] Spies, M., J. *Acoust. Soc. Am.* **110**, 68-79 (2001)
[4] Ding, D., Zhang, Y., Liu, J., J. *Acoust. Soc. Am.* **113**, 3043-3048 (2003)
[5] Spies, M., Ultrasonic Field Modeling for Immersed Components Using Gaussian Beam Superposition, *Ultrasonics,* submitted for publication
[6] Norris, A.N., *Acta Mechanica* **71**, 95-114 (1988)
[7] Spies, M., *J. Acoust*. Soc. Am. **95**, 1748-1760 (1994)
[8] Spies, M., Feist, W.D., Validation of Gaussian Beam Superposition Modeling for Aeroengine Component Inspection, *Ultrasonics*, in preparation